

# Structure of a Compact Peptide from Staphylococcal Nuclease Determined by Circular Dichroism and NMR Spectroscopy<sup>†</sup>

Mark W. Maciejewski<sup>‡</sup> and Micheal H. Zehfus\*

*Division of Medicinal Chemistry and Pharmacognosy, College of Pharmacy, and Department of Biochemistry, College of Biological Sciences, The Ohio State University, Columbus, Ohio 43210*

*Received November 17, 1994; Revised Manuscript Received March 3, 1995<sup>®</sup>*

**ABSTRACT:** Compact regions in proteins are thought to correspond to domains. If this is true, the structure of a compact region excised from a protein should closely resemble the structure in the intact protein. To test this theory, a compact peptide corresponding to residues 129–142 of staphylococcal nuclease (Ac-EAQAKKEKLNWS-NH<sub>2</sub>) was synthesized and its solution structure determined using circular dichroism (CD) and 2D NMR. In aqueous solution, the peptide exhibits CD spectra characteristic of a nascent helix. This nascent helical structure is stabilized by the addition of 2,2,2-trifluoroethanol. Under these conditions, the chemical shift indexes of the <sup>1</sup>H $\alpha$  and <sup>13</sup>C $\alpha$  resonances, temperature coefficients of amide protons, and NOE constraints are all consistent with the peptide's structure being a helix–turn. This structure is almost identical to that found in the intact protein.

The framework model of protein folding states that folding begins with the formation of local regions of fluctuating secondary structure (Anfinsen & Scheraga, 1975). These local regions of secondary structure act as nucleation sites that pack together, probably due to hydrophobic interactions, to form more complex units. In the last step, water molecules are removed from the core allowing interior side chains to pack together into the final tertiary structure (Baldwin, 1989). If this model is correct, local regions that act as nucleation sites should contain native-like structure when cleaved from the intact protein. Several small peptides with nonrandom structure that might act as nucleation sites have been found (Brown & Klee, 1971; Dyson et al., 1988a,b; Blanco et al., 1991; Sancho et al., 1992; Ikura et al., 1993), but it is not easy to predict the presence of such a peptide from its sequence.

Structural domains are regions of proteins that fold spontaneously, even when removed from the rest of the protein. Several studies have linked the presence of domains with regions of the protein that are physically compact. Zehfus has proposed that compactness can be quantitated using a normalized measure of surface area and has identified compact domains using this algorithm (Zehfus & Rose, 1986; Zehfus, 1987, 1994). Physically compact units come in many sizes. Large compact units correspond well with major structural domains, while midsize compact units appear to be subdomains. The smallest compact units contain only 10–20 residues and are too small to be domains or subdomains. One interesting hypothesis is that these smallest “domains” may be folding nucleation sites.

To test if compact units found using this method are true structural entities, staphylococcal nuclease was subjected to compact unit analysis, and several of the most compact peptides were identified. One of the most compact units from staphylococcal nuclease contains residues 129–142 of this protein<sup>1</sup> (peptide B). Here we have synthesized a peptide corresponding to this region, and using CD and NMR, we have found the peptide's solution structure consists of a helix–turn similar to that in the intact protein.

## MATERIALS AND METHODS

Peptide B (129–142) of staphylococcal nuclease was synthesized on an Applied Biosystems 430A solid phase peptide synthesizer using *t*-Boc chemistry (Merrifield, 1963). The N- and C-termini were acetylated and aminated, respectively, to block charge effects. The peptide was purified by preparative HPLC on a reverse phase C8 column using a gradient from 0% to 60% acetonitrile in 0.1% TFA developed over 30 min. The peptide was determined to be >95% pure by analytical HPLC, and the amino acid composition was confirmed by amino acid analysis.

CD spectra were recorded at 5 °C on a Jasco J-500A spectropolarimeter equipped with a computer interface (interface software provided by W. C. Johnson, Jr.). Ellipticity was calibrated daily using a 26.69 mM *d*-10-camphor-sulfonic acid solution at 290.5 nm ( $\Delta\epsilon = +2.36$ ) and 192.5 nm ( $\Delta\epsilon = -4.90$ ). Samples typically contained 0.22 mM

<sup>†</sup> This work was supported by Grant GM46664 from the National Institutes of Health. Equipment used was funded in part by NIH Grants 1 S10 RR-01458-01A1 and 1 S10 RR-08299-01 and NSF Grant BIR-9221639, at The Ohio State University Chemical Instrumentation Center.

\* Author to whom correspondence should be addressed at Division of Medicinal Chemistry and Pharmacognosy, College of Pharmacy.

<sup>‡</sup> Department of Biochemistry, College of Biological Sciences.

<sup>®</sup> Abstract published in *Advance ACS Abstracts*, April 15, 1995.

<sup>1</sup> Abbreviations: CD, circular dichroism; NMR, nuclear magnetic resonance spectroscopy; 2D, two-dimensional; 1D, one-dimensional; TFE, 2,2,2-trifluoroethanol; NOE, nuclear Overhauser enhancement; peptide B, residues 129–142 of staphylococcal nuclease; *t*-Boc, *tert*-butoxyloxycarbonyl; HPLC, high-performance liquid chromatography; TFA, trifluoroacetic acid; TSP, 3-(trimethylsilyl)propionate-2,2,3,3-*d*<sub>4</sub>; ppm, parts per million; TPPI, time proportional phase incrementation; DQF-COSY, double-quantum-filtered correlated spectroscopy; TOCSY, total correlated spectroscopy; ROESY, rotating frame nuclear Overhauser effect spectroscopy; HMQC, single-bond heteronuclear correlation spectroscopy; Gu-HCl, guanidinium hydrochloride; ppb, parts per billion; Glx, glutamic acid or glutamine; BPTI, bovine pancreatic trypsin inhibitor.

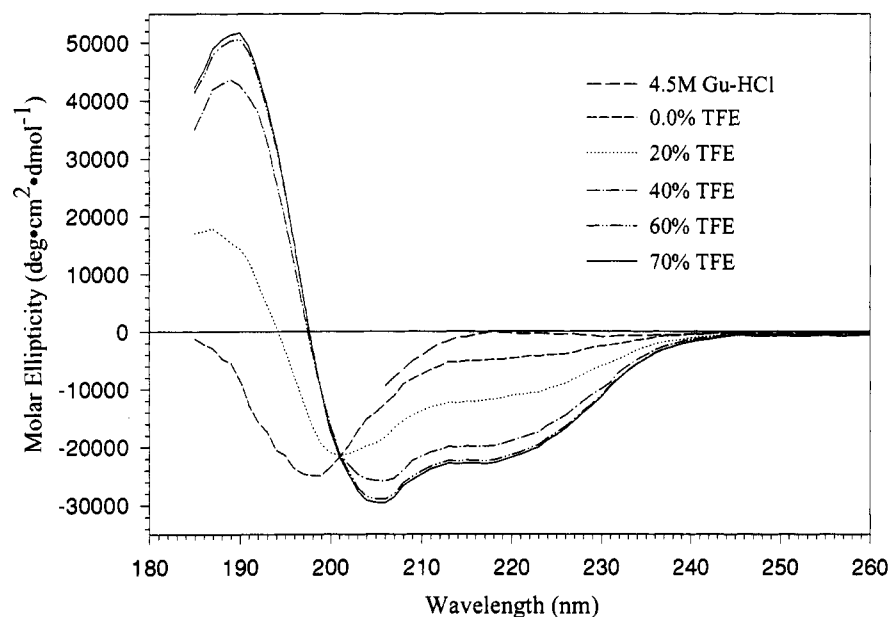


FIGURE 1: CD spectra of peptide B in 4.5 M Gu-HCl, 100% H<sub>2</sub>O, 20% TFE, 40% TFE, 60% TFE, and 70% TFE. All spectra were recorded in 10 mM citrate buffer, pH 4.0, at 5 °C. Sample concentration was 0.22 mM. Data was collected at 1 nm intervals taking 7000 points/nm with a slit width of 2 nm.

peptide, 10 mM citrate buffer, and various amounts of TFE at pH 4.0. Peptide concentrations were determined by absorbance of Trp at 280 nm in H<sub>2</sub>O using 5559 M<sup>-1</sup> cm<sup>-1</sup> as an extinction coefficient (Mihalyi, 1968).

A 3.5 mM NMR sample was prepared by dissolving the peptide in water, adjusting the pH to 4.0 with NaOH and HCl, and then adding TFE-*d*<sub>3</sub> to give a 40% (v/v) solution. NMR data were recorded on a Bruker AMX 500 or AMX 600 spectrometer at 12 °C using sodium 3-(trimethylsilyl)-propionate-2,2,3,3-*d*<sub>4</sub> (TSP) as an internal standard, assigning a 0.0 ppm shift for both <sup>1</sup>H and <sup>13</sup>C measurements. All experiments were recorded in phase sensitive mode using TPPI for quadrature detection in the *t*<sub>1</sub> dimension (Redfield & Kunz, 1975; Marion & Wüthrich, 1983). The water proton signal was suppressed by selective irradiation during the relaxation delay (typically 2 s). Double-quantum-filtered correlation spectroscopy (DQF-COSY) (Piantini et al., 1982; Rance et al., 1983), total correlation spectroscopy (TOCSY) (Braunschweiler & Ernst, 1983; Bax & Davis, 1985), and rotating frame nuclear Overhauser effect spectroscopy (ROESY) (Bothner-By et al., 1984) experiments were recorded with 2K points in *f*<sub>2</sub> with 512 *t*<sub>1</sub> values and a sweep width of 12 ppm. Single-bond heteronuclear correlation (HMQC) (Müller, 1979; Bax et al., 1983; Cavanagh & Keeler, 1988) experiments were taken with a 120 ppm sweep width in *f*<sub>1</sub>. Data were processed on a Indigo workstation (Silicon Graphics, Inc., Mountain View, CA) using Felix 2.30 (Biosym Technologies, San Diego, CA). All data were zero filled in both dimensions to give a 2K × 1K real matrix. A linear prediction of the first data point was performed before *f*<sub>2</sub> Fourier transform, and a base line correction was used to remove any D/C offset. TOCSY experiments were typically recorded with an 80 ms spin-lock and ROESY spectra with a 150 or 250 ms spin-lock.

## RESULTS

Figure 1 shows the CD spectra of peptide B both in aqueous solution with 4.5 M guanidinium chloride (Gu-HCl)

and in mixtures of water and TFE at 5 °C, pH 4.0. The spectrum in 100% H<sub>2</sub>O shows a typical random coil line shape with a minimum at 199 nm but contains a small negative band ( $[\theta]_{222} = -4200^\circ \text{ cm}^2 \text{ dmol}^{-1}$ ) at 222 nm. The addition of 4.5 M Gu-HCl reduces the negative ellipticity at 222 nm ( $[\theta]_{222} = -380^\circ \text{ cm}^2 \text{ dmol}^{-1}$ ), indicating that a small amount of nascent helix exists in aqueous solution. The addition of up to 60% TFE leads to an increase in the negative ellipticity at 222 nm ( $[\theta]_{222} = -20\,200^\circ \text{ cm}^2 \text{ dmol}^{-1}$ ), demonstrating a stabilization of the nascent helix. CD spectra of peptide B were also determined at pH 4.0, 7.0, and 10.0 in a 40% TFE solution at 5 °C; no differences were observed.

NMR resonance assignments were made in 40% TFE, pH 4.0, at 12 °C. This pH was chosen to minimize the exchange rates of the amide protons. DQF-COSY and TOCSY spectra were used to identify spin systems, and ROESY spectra were used to make the sequential assignments (Wüthrich, 1986). The <sup>13</sup>C assignments were made from a natural abundance HMQC experiment. Table 1 lists all resonance assignments for peptide B. To assure that no aggregation was occurring, especially at the high concentrations needed for NMR, CD spectra of peptide B in 40% TFE, pH 4.0, at 5 °C were taken over a concentration range of 11 μM to 3.5 mM. No dependence of ellipticity with concentration was observed.

Figure 2 shows the chemical shift index for both the <sup>1</sup>Hα and <sup>13</sup>Cα resonances. The values were determined by subtracting random coil chemical shift values from observed chemical shifts (Wishart et al., 1992). To avoid changes in chemical shift due to solvent, <sup>13</sup>Cα random coil values were determined in 30% TFE (Thanabal et al., 1994). Values at 40% TFE are not expected to be significantly different.

The temperature dependence of the amide proton chemical shifts of peptide B were studied in a series of 1D and 2D NMR experiments taken from 5 to 39 °C at 2 °C intervals. The chemical shifts all varied linearly with temperature. Temperature coefficients (slopes) were calculated by the method of least squares from a temperature vs chemical shift

Table 1: Resonance Assignments (ppm) of Peptide B in 40% TFE at 12 °C (Relative to TSP)

	NH	$\alpha$	$\beta$	$\gamma$	other	$^{13}\text{C}\alpha$	$^{13}\text{C}\beta$	$^{13}\text{C}\gamma$	other
terminal $\text{CH}_3$					2.14				25.4
Glu 129	8.46	4.16	2.11	2.49		59.0	29.5		
			2.14	2.53					
Ala 130	8.57	4.16	1.47			55.7	19.2		
Gln 131	8.22	4.11	2.16	2.41	N $\delta$ 6.84	59.4	29.5	34.8	
			2.12	2.48	N $\delta'$ 7.44				
Ala 132	8.07	4.17	1.51			55.7	19.2		
Lys 133	8.13	4.07	1.62	1.44	$\delta$ 1.72	59.8	26.3	26.2	$\delta$ 30.4
			1.92		$\epsilon$ 2.98		33.6		$\epsilon$ 43.2
Lys 134	8.07	4.15	1.56	1.43	$\delta$ 1.70	59.2	26.3	26.2	$\delta$ 30.4
			1.90		$\epsilon$ 2.97		33.7		$\epsilon$ 43.2
Glu 135	8.16	4.22	2.19	2.52		58.7	29.3	34.1	
			2.62						
Lys 136	7.97	4.09	1.59	1.46	$\delta$ 1.72	59.67	26.3	26.2	$\delta$ 30.4
			1.95		$\epsilon$ 2.99		33.6		$\epsilon$ 43.2
Leu 137	8.03	4.31	1.64	1.78	$\delta$ 0.95	57.3	43.3	28.0	$\delta$ 25.6
			1.79		$\delta'$ 0.92				$\delta'$ 24.0
Asn 138	8.23	4.62	2.85		N $\delta$ 6.84	55.3	39.7		
					N $\delta'$ 7.55				
Ile 139	7.90	4.02	1.84	1.04	$\gamma\text{CH}_3$ 0.79	64.0	39.6	28.4	$\gamma\text{CH}_3$ 17.9
				1.34	$\delta$ 0.81			28.5	$\delta$ 14.0
Trp 140	8.14	4.68	3.33		$\delta_1$ 7.28	59.1	30.4		$\delta_1$ 127.6
			3.43		n $\epsilon$ 1 9.99				
					$\epsilon_3$ 7.69				$\epsilon_3$ 121.7
					$\zeta_1$ 7.50				$\zeta_1$ 115.4
					$\zeta_2$ 7.17				$\zeta_2$ 122.8
					$\eta$ 7.25				$\eta$ 125.4
Ser 141	7.95	4.34	3.86			59.8	65.0		
			3.96						
terminal $\text{NH}_2$					7.08				

plot. Figure 3 shows the variation of temperature coefficients with the peptide sequence. The line at 6.0 ppb/K shows the range of values measured for amide protons of random coil peptides (Deslauriers & Smith, 1980; Jiménez et al., 1986).

NOESY (ROESY) data were used both to determine sequential assignments and to identify regions of secondary structure. All NOE's typical of secondary structure or relevant to the global fold are listed in Table 2.

## DISCUSSION

As shown in Figure 4, the X-ray structure of staphylococcal nuclease has a helix from residues 129 to 136 and a turn for residues 137–140 (Cotton et al., 1979; Loll & Lattman, 1989). The turn brings residues 140 and 133 into close proximity. The amide protons of residues 129–132 should not be hydrogen bonded because they are the initial four residues of the helix. Likewise, the amide protons of 139–140 should not be hydrogen bonded because they are located in the turn with their amide protons exposed. All other amide protons are hydrogen bonded.

In 100%  $\text{H}_2\text{O}$ , peptide B has a CD spectrum with a minimum at 199 nm consistent with a largely random structure; however, this structure is not entirely denatured. The negative ellipticity of  $-4200^\circ \text{ cm}^2 \text{ dmol}^{-1}$  at 222 nm indicates the presence of roughly 10% helix, based on a 100% reference value of  $-40\,600^\circ \text{ cm}^2 \text{ dmol}^{-1}$  (Merutka et al., 1991). The addition of 4.5 M Gu-HCl decreases the negative ellipticity at 222 nm to  $-380^\circ \text{ cm}^2 \text{ dmol}^{-1}$ , indicating the complete unfolding of the helix. This change at 222 nm between nondenaturing and denaturing conditions demonstrates that some helix persists in aqueous solution and peptide B has a propensity for helix formation.

It has been shown that TFE stabilizes nascent helical conformation without indiscriminately inducing helix elsewhere in the molecule (Seqawa et al., 1991; Dyson et al.,

1992a,b; Sancho et al., 1992). Thus, TFE was used as a cosolvent to stabilize the nascent helix. As shown in Figure 1, the negative ellipticity at 222 nm increases with increasing TFE concentration until 60% TFE, after which further addition makes no appreciable change. At 60% TFE, only about 50% of the peptide is helical, consistent with the structure of the peptide in the native protein. Figure 1 also shows an isodichroic point at 201 nm that demonstrates a two-state transition between random coil and helical structure (Dyson et al., 1988b). To further study peptide B by NMR, 40% TFE was used because the peptide was not sufficiently soluble at higher TFE concentrations.

Despite a large amount of overlap of the Lys and Glx side chains, full assignments for all protons of peptide B were determined (Table 1). This was accomplished primarily using an 80 ms TOCSY experiment that showed almost every connectivity within each spin system. The NH- $\beta$ , - $\gamma$ , - $\delta$ , and - $\epsilon$  crosspeaks of the Lys and Glx spin systems were especially helpful with the assignment procedure. A natural abundance HMQC experiment allowed the determination of a majority of the  $^{13}\text{C}$  resonances (Table 1).

Recently, chemical shifts have become increasingly important in the determination of secondary structure. Most notable are the tendencies of the  $^1\text{H}\alpha$  and  $^{13}\text{C}\alpha$  resonances to adopt characteristic shifts depending on the secondary structure. When in a helix, the  $^1\text{H}\alpha$  resonances experience an upfield shift of approximately 0.4 ppm while the  $^{13}\text{C}\alpha$  resonances experience a downfield shift of about 4.0 ppm. Conversely, the  $^1\text{H}\alpha$  resonances have a downfield shift and the  $^{13}\text{C}\alpha$  resonances an upfield shift when in a  $\beta$ -sheet (Wishart et al., 1991). The chemical shift indexes for both the  $^1\text{H}\alpha$  and  $^{13}\text{C}\alpha$  resonances are plotted in Figure 2. Consistent with helix formation for residues 129–136, the chemical shift indexes for these residues show an upfield shift for the  $^1\text{H}\alpha$  resonances and a downfield shift for the  $^{13}\text{C}\alpha$  resonances. For residues 137–141, the  $^1\text{H}\alpha$  resonances show both upfield and downfield shifts and the  $^{13}\text{C}\alpha$  resonances have a small downfield shift. However, the downfield shift of the  $^{13}\text{C}\alpha$  resonances of residues 137–141 is less than that observed for residues 129–136. Thus, the chemical shift data yield no strong indication of the secondary structure for residues 137–141.

The dependencies of amide proton chemical shift with temperature, as measured by the temperature coefficient, may also be used to identify secondary structure. Solvent-protected amide protons have a lower temperature coefficient than solvent-exposed amide protons. Solvent accessibility of the amide protons was determined by the magnitude of their temperature coefficients (Figure 3). Temperature coefficients for random coil peptides with exposed amide protons are in the range of 6–12 ppb/K (Deslauriers & Smith, 1980; Jiménez et al., 1986). Clearly, residues 131–134, 136, and 138 are all solvent protected and likely to be involved in hydrogen bonds, while residues 129, 130, 139, and 140 are all above 10 ppb/K and must be exposed to solvent. Residues 135, 137, and 141 have temperature coefficients slightly above the 6 ppb/K threshold and are thought to be either exposed or only partially protected. Consistent with the native structure, where residues 139 and 140 are in a turn, the temperature coefficients of residues 139 and 140 are well into the random coil range, showing the helix is terminated before 139.

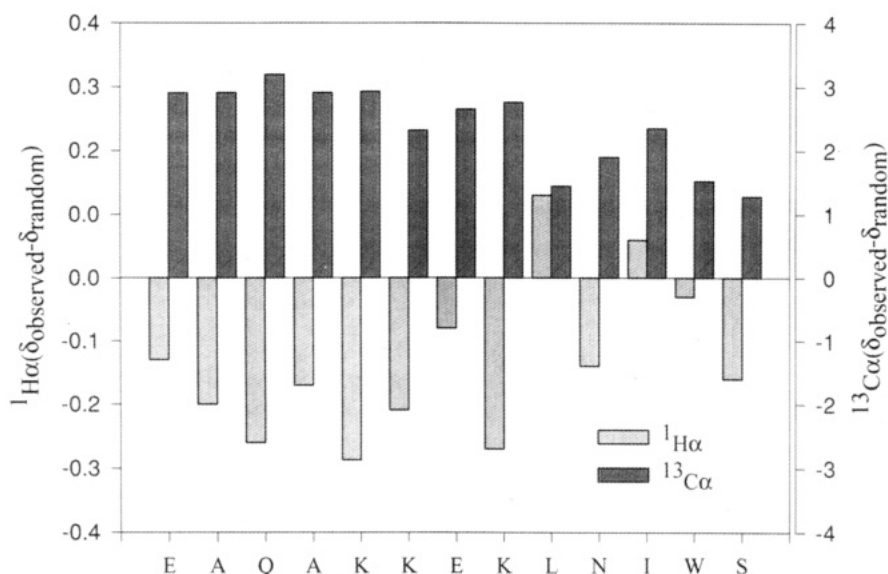


FIGURE 2: Chemical shift indexes for both  $^1\text{H}\alpha$  and  $^{13}\text{C}\alpha$  resonances as a function of residue number for peptide B. Values were determined by subtraction of the corresponding random coil chemical shift from the measured value.  $^{13}\text{C}\alpha$  random coil values were taken in 30% TFE.

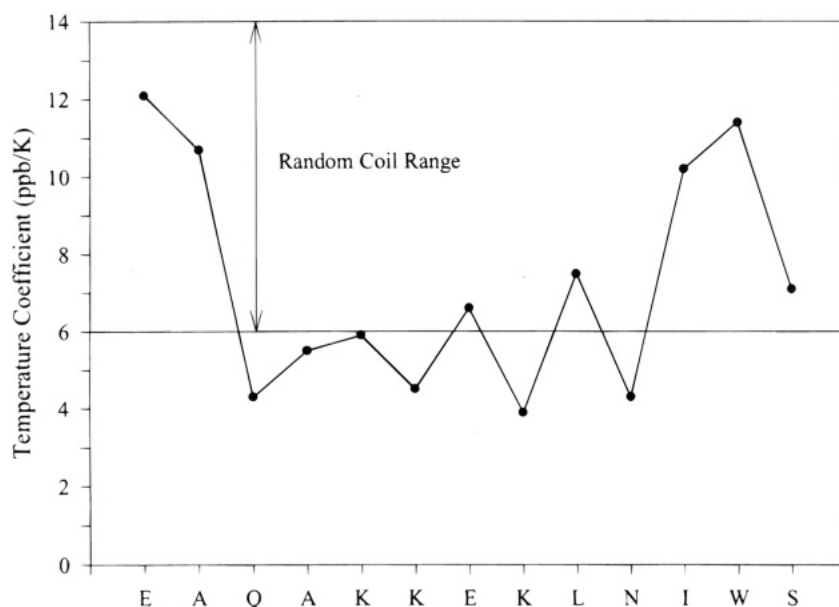


FIGURE 3: Temperature coefficients of the amide protons as a function of residue number for peptide B. Values were determined by taking the absolute value of the slope from a chemical shift vs temperature plot for the amide protons. The range measured for random coil values is also shown.

Table 2: Summary of NOE Connectivities for Peptide B in 40% TFE as 12 °C

	E	A	Q	A	K	K	E	K	L	N	I	W
	129	130	131	132	133	134	135	136	137	138	139	140
dNN $i, i+1$	■	■	■	★	★	★	■		■		■	■
dαN $i, i+1$		■	■			■	■		■	■	■	■
dβN $i, i+1$	■	■	■	■			■		■	■	■	■
dαN $i, i+2$										■		
dαβ $i, i+3$	★	★	★	★	★		■		■	■		
d $i, i+5$						■						

■ - NOE is present  
 ★ - Cannot determine due to spectral overlap

The temperature coefficients of residues 131 and 132 show them to be solvent protected. This is curious because they are at positions 3 and 4 of the helix and should be exposed.

The most likely explanation is that a bifurcated hydrogen bond exists between the carbonyl of the acetate blocking group and the amide protons of residues 131 and 132. Such capping interactions have been observed previously between the carbonyl of the acetate group and residue 3 or 4 of the helix but never to both residues 3 and 4 simultaneously (Chakrabarty et al., 1993; Miick et al., 1993; Doig et al., 1994).

The presence of a helix for residues 129–136 and a turn for residues 137–141 is clearly confirmed in the NOE data. Table 2 shows all inter-residue NOE's used to identify the secondary structure and global fold of the peptide. dNN  $i, i+1$  connectivities are seen in helices and some turns but not in extended conformations. dNN  $i, i+1$  NOE's are found for all residues except 136 and 138. The string of

<sup>2</sup> dNN  $i, i+1$ : denotes a NOE interaction between two amide protons that are one residue apart.

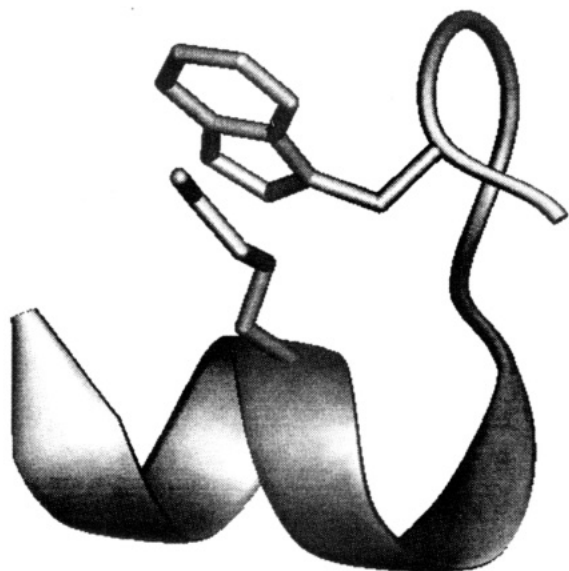


FIGURE 4: Native secondary structure of peptide B, shown as a cartoon diagram. The N-terminus is located on the left and the C-terminus on the right. A helix is shown from residues 129 to 136, depicted as a ribbon, and a turn from residues 137 to 141, shown as a tube. Side chain atoms of Lys 133 and Trp 140 are also shown to demonstrate their close proximity due to the C-terminal turn.

dNN  $i, i + 1$  NOE's from residues 129 to 135, which break at 136 and 138, is consistent with a helix which terminates at residue 136, while the dNN  $i, i + 1$  NOE's of residues 137, 139, and 140 demonstrate that the C-terminus is not in an extended conformation.  $\alpha$ N  $i, i + 1$  and  $\delta$  $\beta$ N  $i, i + 1$  NOE's are found in all types of secondary structure, although they are strongest in sheets. Nine of the possible 12  $\alpha$ N  $i, i + 1$  and  $\delta$  $\beta$ N  $i, i + 1$  connectivities are found spread through the entire sequence. While this is consistent with an ordered structure, it does not indicate the precise type of secondary structure.  $\alpha\beta$   $i, i + 3$  NOE's are another interaction diagnostic of helices; unfortunately, the high degree of resonance overlap of the Ala's, Glx's, and Lys's made it impossible to uniquely identify many of these interactions.

The  $\alpha$ N  $i, i + 2$  NOE present between residue 138 and 140 is a good indication of a turn at the C-terminus. The presence of this C-terminal turn is confirmed by two long range NOE's between residues 134 and 139. Since NOE interactions must be shorter than 5.5 Å, these two NOE's could only be found if a turn has occurred somewhere between these two residues. The lack of any NOE's from residue 136 to any C-terminal residue also makes residue 136 a likely breaking point between the helix and the turn.

In conclusion, peptide B contains a nascent helical structure that can be stabilized with the addition of TFE. When stabilized, the CD spectra, chemical shift indexes, temperature coefficients, and NOE data all show the presence of a helix between residues 129 and 136 and are consistent with the presence of a turn in the C-terminal region. This turn is convincingly demonstrated by the NOE interactions between residues 134 and 139. The structure of this isolated peptide thus closely resembles its structure in the native protein. This finding corroborates the hypothesis that small compact units fold to native-like structures and may serve as folding nucleation sites.

The target sequence for this peptide was chosen by identifying a region in staphylococcal nuclease that has a small surface area for its enclosed volume (Zehfus & Rose, 1986). While this is the first direct test that this definition of compactness actually identifies structural entities, it should be noted that other peptides with defined solution structures also fit this model. The C peptide of ribonuclease (1–13) contains a native-like structure in solution (Brown & Klee, 1971) and residues 2–12 are compact by this definition (Zehfus & Rose, 1986). The P $\alpha$ P $\beta$  peptide (20–33 + 43–58) of BPTI has a structure nearly identical to the native protein (Oas & Kim, 1988) and corresponds closely to the 20–33 + 43–56 compact binary discontinuous unit (Zehfus, 1994). Thus the tie between compactness and stable solution structure is seen in data from different labs and systems and highlights compactness, as measured using normalized surface areas, an important structural parameter.

#### ACKNOWLEDGMENT

We thank Dr. John Lowbridge for synthesizing the peptide and Dr. Charles E. Cottrell for his help in running the FT-NMR spectra. We also thank Dr. W. C. Johnson, Jr. (Department of Biochemistry and Biophysics, Oregon State University) for the software to run the computer interface on the spectropolarimeter.

#### REFERENCES

- Anfinsen, C. B., & Scheraga, H. A. (1975) *Adv. Protein Chem.* 29, 205–300.
- Baldwin, R. L. (1989) *TIBS* 14, 291–294.
- Bax, A., & Davis, D. G. (1985) *J. Magn. Reson.* 65, 355–360.
- Bax, A., Griffey, R. H., & Hawkins, B. L. (1983) *J. Magn. Reson.* 55, 301–315.
- Blanco, F. J., Jiménez, M. A., Rico, M., Santoro, J., Herranz, J., & Nieto, J. L. (1991) *Eur. J. Biochem.* 200, 345–351.
- Bothner-By, A. A., Stephens, R. L., Lee, J. M., Warren, C. D., & Jeanloz, R. W. (1984) *J. Am. Chem. Soc.* 101, 811–813.
- Braunschweiler, L., & Ernst, R. R. (1983) *J. Magn. Reson.* 53, 521–528.
- Brown, J. E., & Klee, W. A. (1971) *Biochemistry* 10, 470–476.
- Cavanagh, J., & Keeler, J. (1988) *J. Magn. Reson.* 77, 356–362.
- Chakrabarty, A., Doig, A. J., & Baldwin, R. L. (1993) *Proc. Natl. Acad. Sci. U.S.A.* 90, 11332–11336.
- Cotton, F. A., Hazen, E. E., Jr., & Legg, M. J. (1979) *Proc. Natl. Acad. Sci. U.S.A.* 76, 2551–2555.
- Deslauriers, R., & Smith, I. C. P. (1980) in *Biological magnetic resonance*, (Berliner, L. J., & Reuben, J., Eds.) Vol. 2, pp 243–344, Plenum, New York.
- Doig, A. J., Chakrabarty, A., Klingler, T. M., & Baldwin, R. L. (1994) *Biochemistry* 33, 3396–3403.
- Dyson, H. J., Rance, M., Houghten, R. A., Lerner, R. A., & Wright, P. E. (1988a) *J. Mol. Biol.* 201, 161–200.
- Dyson, H. J., Rance, M., Houghten, R. A., Wright, P. E., & Lerner, R. A. (1988b) *J. Mol. Biol.* 201, 201–217.
- Dyson, H. J., Merutka, G., Waltho, J. P., Lerner, R. A., & Wright, P. E. (1992a) *J. Mol. Biol.* 226, 795–817.
- Dyson, H. J., Sayre, J. R., Merutka, G., Shin, H.-C., Lerner, R. A., & Wright, P. E. (1992b) *J. Mol. Biol.* 226, 819–835.
- Ikura, T., Gō, N., Kohda, D., Inagaki, F., Yanagawa, H., Kawabata, M., Kawabata, S., Iwanaga, S., Noguti, T., & Gō, M. (1993) *Proteins* 16, 341–356.
- Jiménez, M. A., Nieto, J. L., Rico, M., Santoro, J., Herranz, J., & Bermejo, F. J. (1986) *J. Mol. Struct.* 143, 435–438.
- Loll, P. J., & Lattman, E. E. (1989) *Proteins* 5, 183–201.
- Marion, D., & Wüthrich, K. (1983) *Biochem. Biophys. Res. Commun.* 113, 967–974.
- Merrifield, R. B. (1963) *J. Am. Chem. Soc.* 85, 2149–2154.

- Merutka, G., Shalongo, W., & Stellwagen, E. (1991) *Biochemistry* 30, 4245–4248.
- Mihalyi, E. (1968) *J. Chem. Eng. Data* 13, 179–182.
- Miick, S. M., Casteel, K. M., & Millhauser, G. L. (1993) *Biochemistry* 32, 8014–8021.
- Müller, L. (1979) *J. Am. Chem. Soc.* 101, 4481–4484.
- Oas, T. G., & Kim, P. S. (1988) *Nature* 336, 42–48.
- Piantini, U., Sørensen, O. W., & Ernst, R. R. (1982) *J. Am. Chem. Soc.* 104, 6800–6801.
- Rance, M., Sørensen, O. W., Bodenhausen, G., Wagner, G., Ernst, R. R., & Wüthrich, K. (1983) *Biochem. Biophys. Res. Commun.* 117, 479–485.
- Redfield, A. G., & Kunz, S. D. (1975) *J. Magn. Reson.* 19, 250–254.
- Sancho, J., Neira, J. L., & Fersht, A. R. (1992) *J. Mol. Biol.* 224, 749–758.
- Seqawa, S. I., Fukuno, T., Fujiwara, K., & Noda, Y. (1991) *Biopolymers* 31, 497–509.
- Thanabal, V., Omecinsky, D. O., Reily, M. D., & Cody, W. L. (1994) *J. Biomol. NMR* 4, 47–59.
- Wishart, D. S., Sykes, B. D., & Richards, F. M. (1991) *J. Mol. Biol.* 222, 311–333.
- Wishart, D. S., Sykes, B. D., & Richards, F. M. (1992) *Biochemistry* 31, 1647–1651.
- Wüthrich, K. (1986) *NMR of Proteins and Nucleic Acids*, Wiley & Sons, New York.
- Zehfus, M. H. (1987) *Proteins* 2, 90–110.
- Zehfus, M. H. (1994) *Protein Eng.* 7, 335–340.
- Zehfus, M. H., & Rose, G. D. (1986) *Biochemistry* 25, 5759–5765.

BI942675I